



ARISTOTELIO UNIVERSITY OF THESSALONIKI Polytechnic School
Department of Mechanical Engineering
Laboratory of FLUID & TURBINE ENGINEERING

COMPUTATIONAL FLUID MECHANICS

THREE – SIDED LID DRIVEN CLOSE CAVITY

Aythor : Diogenis Tsichlakis

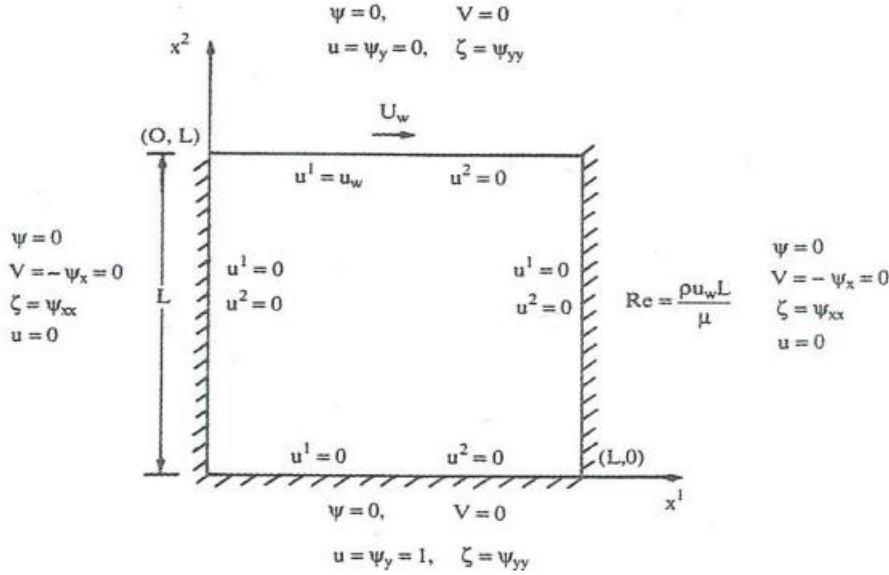
Thessaloniki, May 2022

CONTENTS

1 INTRODUCTION	3
2. PROBLEM IDENTIFICATION	4
2.1 Grid Construction	4
2.2Complex Method – Discretization of Equations	6
2.3 Discretion of Bountary Conditions.....	12
3. PROCEDURE FOR CALCULATING FLOW FIELD.....	13
3.1 Relaxation Techniques	13
3.2 Explicit Algorithm.....	14
3.3 Results and Comparison.....	17
4. GRID INDEPENDENCE STUDY	24
5. SOLUTION WITH DIFFERENT BOUNDART CONDITIONS.....	27
5.1 Differentiate, Solve and Compare	27
6. BIBLIOGRAPHY	28

1 INTRODUCTION

In this work we are asked to calculate incompressible fluid flow inside a rectangular cavity. The walls of the pit remain stationary, except for the upper wall which moves with speed in the x direction. Due to the movement of this upper wall and its contact with the fluid inside the cavity, we have agitation of the fluid. This stirring creates eddies depending on the Reynolds number, the flow. The sketch of the problem is shown in Figure 1. U_w



Shape1. Cavity of rectangular cross-section and problem boundary conditions

The equations governing our problem are:

- Turbulence conservation equation:

$$\frac{\partial \zeta}{\partial t} + u \frac{\partial \zeta}{\partial x} + v \frac{\partial \zeta}{\partial y} = Re^{-1} \left(\frac{\partial^2 \zeta}{\partial x^2} + \frac{\partial^2 \zeta}{\partial y^2} \right)$$

Using the flow function expressed in Cartesian coordinates:

$$u = \frac{\partial \psi}{\partial y} \quad v = -\frac{\partial \psi}{\partial x}$$

The above equation comes in the form:

$$\frac{\partial \zeta}{\partial t} = -\frac{\partial \psi}{\partial y} \frac{\partial \zeta}{\partial x} + \frac{\partial \psi}{\partial x} \frac{\partial \zeta}{\partial y} + Re^{-1} \left(\frac{\partial^2 \zeta}{\partial x^2} + \frac{\partial^2 \zeta}{\partial y^2} \right) \quad (1)$$

- We also have the equation of the stream function with respect to the vorticity:

$$\frac{\partial^2 \psi}{\partial x^2} + \frac{\partial^2 \psi}{\partial y^2} = -\zeta$$

Equation (1) is a parabolic equation, with time-dependent terms $\left(\frac{\partial \zeta}{\partial t}\right)$, while the 2nd equation is an elliptic equation. In general, in problems characterized by these 2 categories of equations, we have the phenomenon with time dependence described by the parabolic equation (1), while the elliptic equations express the phenomena in the steady state.

A frequently applied method to solve such problems is to add a partial derivative with respect to time to the elliptic equation [Ref. 1], so as to turn the whole problem into a parabolic one. With this process, when the steady state is reached, this time derivative becomes zero and thus the original elliptic equation is satisfied. Thus the 2nd of the above equations is transformed into the form: $\left(\frac{\partial \psi}{\partial t}\right)$

$$\frac{\partial^2 \psi}{\partial x^2} + \frac{\partial^2 \psi}{\partial y^2} + \zeta = \frac{\partial \psi}{\partial t} \quad (2)$$

$$\xrightarrow{\text{steady state}} \frac{\partial \psi}{\partial t} = 0 \Rightarrow \frac{\partial^2 \psi}{\partial x^2} + \frac{\partial^2 \psi}{\partial y^2} = -\zeta$$

Equations (1), (2) are in non-dimensionalized form, the importance of non-dimensionalization is reflected in the visualization of the results (and the reduction of numerical errors). In solving these equations we will apply different Reynolds numbers. Even though this number depends on the dimensions of the pit and the velocity of the upper wall, the results we will get will be referred to (diastatization ratio) always in unit values of both the non-diameterized dimension L (L=1) and the non-diameterized velocity. ($U_w = 1$)

Using the above 2 equations that describe the problem, we are asked:

1. Geometric discretization of space (Grid)
2. Problem Discretization in Complex Form
3. Calculation of rheological field using relaxation techniques
4. Visualization of vorticity and vorticity lines for different Re
5. Grid independence study for 3 pairs of dimensions
6. Solving the same problem for reverse movement of the upper wall

Having described the problem we have to solve, we proceed to the analysis and solution. All the algorithms needed to produce the results were written in Python.

2. PROBLEM IDENTIFICATION

2.1 Grid Construction

We begin by discretizing our physical field and constructing the grid in space. Our grid is orthogonal with constant and equal steps in the x and y directions. We introduce the same number of nodes in the 2 directions, in a parameterized way so that during the solution it is possible to change them (nodx and nody). The grid dimensions are the same as the pit dimensions, L height and L length. The form of the mesh is shown in Figure 2. In this figure we also see the boundary conditions of the problem (BCC). For these boundary conditions we have on the 3 stationary walls (right, left and bottom) ($\Delta y = \Delta x$).

$$u = v = 0$$

where from the equations of the flow function it follows and $\frac{\partial \psi}{\partial y}|_{\tau o \chi \omega \mu \alpha} = 0 \Rightarrow \psi = 0$

For the top moving wall we have and $u = \frac{\partial \psi}{\partial y} = U_w, v = 0 \Rightarrow \frac{\partial \psi}{\partial x} = -v \Rightarrow \psi = 0$

For the vorticity on the 4 walls, we recall the equation:

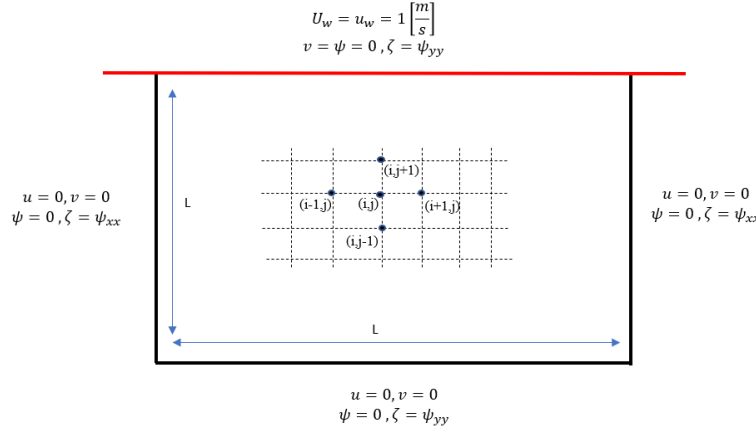
$$\frac{\partial^2 \psi}{\partial x^2} + \frac{\partial^2 \psi}{\partial y^2} = -\zeta$$

From the above (SS) we have that the flow function is constant along the walls, so its change in this direction (of the wall) will be zero. For example on the lower wall we will have ($y=\text{const}$) for the change in the x direction : , so from the equation for the vorticity we have for the lower wall.

With the same rationale, the following are also obtained for the other walls: $\frac{\partial \psi}{\partial x} = 0 \Rightarrow \frac{\partial^2 \psi}{\partial x^2} =$

$$0 \Rightarrow \zeta_{\tau o \chi \omega \mu \alpha} = -\frac{\partial^2 \psi}{\partial y^2}$$

$$\left\{ \begin{array}{l} \text{Upper Wall : } \frac{\partial^2 \psi}{\partial x^2} = 0 \Rightarrow \zeta_{wall} = -\frac{\partial^2 \psi}{\partial y^2} \\ \text{Lower Wall : } \frac{\partial^2 \psi}{\partial x^2} = 0 \Rightarrow \zeta_{wall} = -\frac{\partial^2 \psi}{\partial y^2} \\ \text{Right Wall : } \frac{\partial^2 \psi}{\partial y^2} = 0 \Rightarrow \zeta_{wall} = -\frac{\partial^2 \psi}{\partial x^2} \\ \text{Left Wall : } \frac{\partial^2 \psi}{\partial y^2} = 0 \Rightarrow \zeta_{wall} = -\frac{\partial^2 \psi}{\partial x^2} \end{array} \right. \quad (I)$$



Shape2. Geometric Discretization of problem and SS

Let us also say that at time 1 ($t=0$), all variables under study inside the well are zero.

After completing the construction of the grid and the definition of the SS, we proceed to discretize the equations spatially and temporally.

2.2 Complex Method – Discretization of Equations

The flow equations we are interested in will be discretized with finite differences in time and space. The time derivatives will be approximated by forward finite difference, while the partial derivatives with respect to the 1st order x,y coordinates will be approximated by central differences. Finally the 2nd order spatial derivatives are approximated with 2nd order finite differences. The indices for the direction in x-direction, y-direction and time are chosen to be respectively i, j and n . Thus the partial derivative and finite difference relations for a random function A are:

- $\frac{\partial A}{\partial t} = \frac{A_{i,j}^{n+1} - A_{i,j}^n}{\Delta t} + O(\Delta t)$ (forward)
- $\frac{\partial A}{\partial x} = \frac{A_{i+1,j}^n - A_{i-1,j}^n}{2\Delta x} + O(\Delta x^2)$ (Central)
- $\frac{\partial A}{\partial y} = \frac{A_{i,j+1}^n - A_{i,j-1}^n}{2\Delta y} + O(\Delta y^2)$ (Central)
- $\frac{\partial^2 A}{\partial x^2} = \frac{A_{i+1,j}^n - 2A_{i,j}^n + A_{i-1,j}^n}{(\Delta x)^2} + O(\Delta x^2)$ (second order)

$$\circ \quad \frac{\partial^2 A}{\partial y^2} = \frac{A_{i,j+1}^n - 2A_{i,j}^n + A_{i,j-1}^n}{(\Delta y)^2} + O(\Delta y^2) \quad (\text{second order})$$

We now rewrite as a reminder the equations we want to solve:

$$\frac{\partial \zeta}{\partial t} = -\frac{\partial \psi}{\partial y} \frac{\partial \zeta}{\partial x} + \frac{\partial \psi}{\partial x} \frac{\partial \zeta}{\partial y} + Re^{-1} \left(\frac{\partial^2 \zeta}{\partial x^2} + \frac{\partial^2 \zeta}{\partial y^2} \right) \quad (1)$$

$$\frac{\partial^2 \psi}{\partial x^2} + \frac{\partial^2 \psi}{\partial y^2} + \zeta = \frac{\partial \psi}{\partial t} \quad (2)$$

Alternating – Direction – Implicit (ADI)

To solve the above system of equations, due to the non-linearity of the equations and the dependence of the variables under study on 2 spatial and 1 time coordinate, we cannot apply the well-known Crank-Nicolson(CR) method. Applying the CR method will lead to a entangled system of 5 unknowns for which the Thomas algorithm cannot be applied, resulting in the computational burden becoming very large, even prohibitive.

For the solution we will therefore apply the (ADI) method. In essence, this method uses an intermediate (imaginary) time step to solve the equations:

$$n \xrightarrow{1^o} n + \frac{1}{2} \xrightarrow{2^o} n + 1$$

The result of the intermediate step is to solve at each step a system of equations with 3 unknowns (Tridiagonal System) and thus the application of the Thomas algorithm is possible. In essence at each step we discretize our equations in time only in the x or y direction each time. Specifically in the 1st step we discretize the partial derivatives only with respect to x of the 2 equations, in entangled form, so the finite difference for the y direction is written for the initial time (n) during which all field values are considered known. In the 2nd step we discretize the partial derivatives only with respect to y, so we end up with the same process to have a tridiagonal system in which all the terms of the finite differences with respect to y, are written for the time in which the values of the variables of the field were calculated in the previous step. $\left(n + \frac{1}{2}\right)$

Finally to mention that the ADI method has 2nd order accuracy and so the cutoff error is $O[(\Delta t)^2, (\Delta x)^2, (\Delta y)^2]$

Application of ADI Method

We then apply the steps of the ADI method scheme to our own equations and construct the discretized equations, which we will use along the way to calculate our flow field.

We write the finite differences with respect to time and with respect to the x only spatial coordinate for the time instant only for the vorticity equations, so we get the following finite differences: $\left(n + \frac{1}{2}\right)$

$$\circ \quad \frac{\partial \zeta}{\partial t} = \frac{\zeta_{i,j}^{n+\frac{1}{2}} - \zeta_{i,j}^n}{\frac{\Delta t}{2}} + O(\Delta t) \quad (\text{forward})$$

- $\frac{\partial \psi}{\partial t} = \frac{\psi_{i,j}^{n+\frac{1}{2}} - \psi_{i,j}^n}{\frac{\Delta t}{2}} + O(\Delta t)$ (*forward*)
- $\frac{\partial \zeta}{\partial x} = \frac{\zeta_{i+1,j}^{n+\frac{1}{2}} - \zeta_{i-1,j}^{n+\frac{1}{2}}}{2\Delta x} + O(\Delta x^2)$ (*central*)
- $\frac{\partial \zeta}{\partial y} = \frac{\zeta_{i,j+1}^n - \zeta_{i,j-1}^n}{2\Delta y} + O(\Delta y^2)$ (*central*)
- $\frac{\partial \psi}{\partial x} = \frac{\psi_{i+1,j}^n - \psi_{i-1,j}^n}{2\Delta x} + O(\Delta x^2)$ (*central*)
- $\frac{\partial \psi}{\partial y} = \frac{\psi_{i,j+1}^n - \psi_{i,j-1}^n}{2\Delta y} + O(\Delta y^2)$ (*central*)
- $\frac{\partial^2 \zeta}{\partial x^2} = \frac{\zeta_{i+1,j}^{n+\frac{1}{2}} - 2\zeta_{i,j}^{n+\frac{1}{2}} + \zeta_{i-1,j}^{n+\frac{1}{2}}}{(\Delta x)^2} + O(\Delta x^2)$ (*second order*)
- $\frac{\partial^2 \zeta}{\partial y^2} = \frac{\zeta_{i,j+1}^n - 2\zeta_{i,j}^n + \zeta_{i,j-1}^n}{(\Delta y)^2} + O(\Delta y^2)$ (*second order*)

The choice to discretize the vorticity and stream function equations for different times is done to avoid the non-linear terms that would otherwise appear.

We replace the above differences, in (1):

$$\begin{aligned} \frac{\partial \zeta}{\partial t} &= -\frac{\partial \psi}{\partial y} \frac{\partial \zeta}{\partial x} + \frac{\partial \psi}{\partial x} \frac{\partial \zeta}{\partial y} + Re^{-1} \left(\frac{\partial^2 \zeta}{\partial x^2} + \frac{\partial^2 \zeta}{\partial y^2} \right) \Rightarrow \\ \frac{\zeta_{i,j}^{n+\frac{1}{2}} - \zeta_{i,j}^n}{\frac{\Delta t}{2}} &= - \left(\frac{\zeta_{i+1,j}^{n+\frac{1}{2}} - \zeta_{i-1,j}^{n+\frac{1}{2}}}{2\Delta x} \right) \left(\frac{\psi_{i,j+1}^n - \psi_{i,j-1}^n}{2\Delta y} \right) + \left(\frac{\psi_{i+1,j}^n - \psi_{i-1,j}^n}{2\Delta x} \right) \left(\frac{\zeta_{i,j+1}^n - \zeta_{i,j-1}^n}{2\Delta y} \right) \\ &\quad + Re^{-1} \left(\frac{\zeta_{i+1,j}^{n+\frac{1}{2}} - 2\zeta_{i,j}^{n+\frac{1}{2}} + \zeta_{i-1,j}^{n+\frac{1}{2}}}{(\Delta x)^2} + \frac{\zeta_{i,j+1}^n - 2\zeta_{i,j}^n + \zeta_{i,j-1}^n}{(\Delta y)^2} \right) \end{aligned}$$

From the above equation we consider the terms calculated at time n to be known, so we distinguish on the left, unknown terms at time with time step $\left(n + \frac{1}{2}\right) \Delta \tau = \frac{1}{2} \Delta t$

$$\begin{aligned} \frac{\zeta_{i,j}^{n+\frac{1}{2}}}{\frac{\Delta t}{2}} - \frac{\zeta_{i,j}^n}{\frac{\Delta t}{2}} &= -\frac{\zeta_{i+1,j}^{n+\frac{1}{2}}}{2\Delta x} \psi_y + \frac{\zeta_{i-1,j}^{n+\frac{1}{2}}}{2\Delta x} \psi_y + \psi_x \frac{\zeta_{i,j+1}^n}{2\Delta y} - \psi_x \frac{\zeta_{i,j-1}^n}{2\Delta y} + \frac{\zeta_{i+1,j}^{n+\frac{1}{2}} - 2\zeta_{i,j}^{n+\frac{1}{2}} + \zeta_{i-1,j}^{n+\frac{1}{2}}}{Re(\Delta x)^2} \\ &\quad + \frac{\zeta_{i,j+1}^n - 2\zeta_{i,j}^n + \zeta_{i,j-1}^n}{Re(\Delta y)^2} \end{aligned}$$

After numerical operations, we conclude:

$$\Rightarrow A_{i,j}^n \zeta_{i-1,j}^{n+\frac{1}{2}} + B_{i,j}^n \zeta_{i,j}^{n+\frac{1}{2}} + C_{i,j}^n \zeta_{i+1,j}^{n+\frac{1}{2}} = D_{i,j}^n \zeta_{i,j-1}^n + E_{i,j}^n \zeta_{i,j}^n + F_{i,j}^n \zeta_{i,j+1}^n \quad (3)$$

With :

$$\begin{aligned}\Psi_y &= \left(\frac{\psi_{i,j+1}^n - \psi_{i,j-1}^n}{2\Delta y} \right) \\ \Psi_x &= \left(\frac{\psi_{i+1,j}^n - \psi_{i-1,j}^n}{2\Delta x} \right) \\ A_{i,j}^n &= -\frac{\Psi_y}{2\Delta x} - \frac{1}{Re(\Delta x)^2} \\ B &= \frac{2}{\Delta t} + \frac{2}{Re(\Delta x)^2} \\ C_{i,j}^n &= \frac{\Psi_y}{2\Delta x} - \frac{1}{Re(\Delta x)^2} \\ D_{i,j}^n &= \frac{1}{Re(\Delta y)^2} - \frac{\Psi_x}{2\Delta y} \\ E &= \frac{2}{\Delta t} - \frac{2}{Re(\Delta y)^2} \\ F_{i,j}^n &= \frac{1}{Re(\Delta y)^2} + \frac{\Psi_x}{2\Delta y}\end{aligned}$$

Because during the solution, we consider that the values of the variables at time n are known, in the above equation the coefficients for the terms of the tortuosity and the entire right-hand member of equation (3) are considered known. We repeat the same process but this time we write at time $n + \frac{1}{2}$, the partial derivatives with respect to time and the vorticity terms only in the y direction, so we have the following finite differences for time step as before:

- $\frac{\partial \zeta}{\partial t} = \frac{\zeta_{i,j}^{n+1} - \zeta_{i,j}^{n+\frac{1}{2}}}{\frac{\Delta t}{2}} + O(\Delta t) \quad (forward)$
- $\frac{\partial \psi}{\partial t} = \frac{\psi_{i,j}^{n+1} - \psi_{i,j}^n}{\frac{\Delta t}{2}} + O(\Delta t) \quad (forward)$
- $\frac{\partial \zeta}{\partial x} = \frac{\zeta_{i+1,j}^{n+\frac{1}{2}} - \zeta_{i-1,j}^{n+\frac{1}{2}}}{2\Delta x} + O(\Delta x^2) \quad (Central)$
- $\frac{\partial \zeta}{\partial y} = \frac{\zeta_{i,j+1}^{n+1} - \zeta_{i,j-1}^{n+1}}{2\Delta y} + O(\Delta y^2) \quad (Central)$
- $\frac{\partial \psi}{\partial x} = \frac{\psi_{i+1,j}^n - \psi_{i-1,j}^n}{2\Delta x} + O(\Delta x^2) \quad (Central)$
- $\frac{\partial \psi}{\partial y} = \frac{\psi_{i,j+1}^n - \psi_{i,j-1}^n}{2\Delta y} + O(\Delta y^2) \quad (Central)$
- $\frac{\partial^2 \zeta}{\partial x^2} = \frac{\zeta_{i+1,j}^{n+\frac{1}{2}} - 2\zeta_{i,j}^{n+\frac{1}{2}} + \zeta_{i-1,j}^{n+\frac{1}{2}}}{(\Delta x)^2} + O(\Delta x^2) \quad (Second Order)$

$$\circ \quad \frac{\partial^2 \zeta}{\partial y^2} = \frac{\zeta_{i,j+1}^{n+1} - 2\zeta_{i,j}^{n+1} + \zeta_{i,j-1}^{n+1}}{(\Delta y)^2} + O(\Delta y^2) \quad (\text{second order})$$

Substituting in (1) we get:

$$\begin{aligned} \frac{\partial \zeta}{\partial t} &= -\frac{\partial \psi}{\partial y} \frac{\partial \zeta}{\partial x} + \frac{\partial \psi}{\partial x} \frac{\partial \zeta}{\partial y} + Re^{-1} \left(\frac{\partial^2 \zeta}{\partial x^2} + \frac{\partial^2 \zeta}{\partial y^2} \right) \Rightarrow \\ \frac{\zeta_{i,j}^{n+1} - \zeta_{i,j}^{n+\frac{1}{2}}}{\frac{\Delta t}{2}} &= -\left(\frac{\psi_{i,j+1}^n - \psi_{i,j-1}^n}{2\Delta y} \right) \left(\frac{\zeta_{i+1,j}^{n+\frac{1}{2}} - \zeta_{i-1,j}^{n+\frac{1}{2}}}{2\Delta x} \right) + \left(\frac{\psi_{i+1,j}^n - \psi_{i-1,j}^n}{2\Delta x} \right) \left(\frac{\zeta_{i,j+1}^{n+1} - \zeta_{i,j-1}^{n+1}}{2\Delta y} \right) \\ &\quad + Re^{-1} \left(\frac{\zeta_{i+1,j}^{n+\frac{1}{2}} - 2\zeta_{i,j}^{n+\frac{1}{2}} + \zeta_{i-1,j}^{n+\frac{1}{2}}}{(\Delta x)^2} + \frac{\zeta_{i,j+1}^{n+1} - 2\zeta_{i,j}^{n+1} + \zeta_{i,j-1}^{n+1}}{(\Delta y)^2} \right) \end{aligned}$$

From the above equation we consider the terms calculated at the time to be known, so we distinguish on the left unknown terms at the time with time step $\left(n + \frac{1}{2}\right) n + 1\Delta\tau = \frac{1}{2}\Delta t$

$$\Rightarrow AA_{i,j}^n \zeta_{i,j-1}^{n+1} + BB \zeta_{i,j}^{n+1} + CC_{i,j}^n \zeta_{i,j+1}^{n+1} = DD_{i,j}^n \zeta_{i-1,j}^{n+\frac{1}{2}} + EE \zeta_{i,j}^{n+\frac{1}{2}} + FF_{i,j}^n \zeta_{i+1,j}^{n+\frac{1}{2}} \quad (4)$$

Where:

$$\Psi_y = \left(\frac{\psi_{i,j+1}^n - \psi_{i,j-1}^n}{2\Delta y} \right)$$

$$\Psi_x = \left(\frac{\psi_{i+1,j}^n - \psi_{i-1,j}^n}{2\Delta x} \right)$$

$$AA_{i,j}^n = \frac{\Psi_x}{2\Delta y} - \frac{1}{Re(\Delta y)^2}$$

$$BB = \frac{2}{\Delta t} + \frac{2}{Re(\Delta y)^2}$$

$$CC_{i,j}^n = -\frac{\Psi_x}{2\Delta y} - \frac{1}{Re(\Delta y)^2}$$

$$DD_{i,j}^n = \frac{1}{Re(\Delta x)^2} + \frac{\Psi_y}{2\Delta x}$$

$$EE = \frac{2}{\Delta t} - \frac{2}{Re(\Delta x)^2}$$

$$FF_{i,j}^n = \frac{1}{Re(\Delta x)^2} - \frac{\Psi_y}{2\Delta x}$$

Because during the solution, we consider that the values of the variables at time n are known, in the above equation the coefficients for the vorticity terms and the entire right-hand member of equation (4) are considered known.

Thus, the system of equations we conclude for equation (1), using the intermediate step, is:

$$\begin{cases} A_{i,j}^n \zeta_{i-1,j}^{n+\frac{1}{2}} + B \zeta_{i,j}^{n+\frac{1}{2}} + C_{i,j}^n \zeta_{i+1,j}^{n+\frac{1}{2}} = D_{i,j}^n \zeta_{i,j-1}^n + E \zeta_{i,j}^n + F_{i,j}^n \zeta_{i,j+1}^n & (3) \\ AA_{i,j}^n \zeta_{i,j-1}^{n+1} + BB \zeta_{i,j}^{n+1} + CC_{i,j}^n \zeta_{i,j+1}^{n+1} = DD_{i,j}^n \zeta_{i-1,j}^{n+\frac{1}{2}} + EE \zeta_{i,j}^{n+\frac{1}{2}} + FF_{i,j}^n \zeta_{i+1,j}^{n+\frac{1}{2}} & (4) \end{cases} \quad (II)$$

Applying now the same procedure for equation (2), but now discretizing with the intermediate step only the terms of the flow function, we initially have for time n with step: $\Delta\tau = \frac{\Delta t}{2}$

$$\begin{aligned} \frac{\psi_{i,j}^{n+\frac{1}{2}} - \psi_{i,j}^n}{\frac{\Delta t}{2}} - \zeta_{i,j}^n &= \frac{\psi_{i+1,j}^{n+\frac{1}{2}} - 2\psi_{i,j}^{n+\frac{1}{2}} + \psi_{i-1,j}^{n+\frac{1}{2}}}{(\Delta x)^2} + \frac{\psi_{i,j+1}^n - 2\psi_{i,j}^n + \psi_{i,j-1}^n}{(\Delta y)^2} \Rightarrow \\ \left(\frac{1}{(\Delta x)^2}\right) \left(-\psi_{i+1,j}^{n+\frac{1}{2}} + 2\psi_{i,j}^{n+\frac{1}{2}} - \psi_{i-1,j}^{n+\frac{1}{2}}\right) + \frac{\psi_{i,j}^{n+\frac{1}{2}}}{\frac{\Delta t}{2}} &= \zeta_{i,j}^n + \frac{1}{(\Delta y)^2} (\psi_{i,j+1}^n - 2\psi_{i,j}^n + \psi_{i,j-1}^n) + \frac{\psi_{i,j}^n}{\frac{\Delta t}{2}} \\ \Rightarrow \left(-\frac{1}{(\Delta x)^2}\right) \psi_{i+1,j}^{n+\frac{1}{2}} + \left(\frac{2}{(\Delta x)^2} + \frac{2}{\Delta t}\right) \psi_{i,j}^{n+\frac{1}{2}} + \left(-\frac{1}{(\Delta x)^2}\right) \psi_{i-1,j}^{n+\frac{1}{2}} &= \zeta_{i,j}^n + \left(-\frac{1}{(\Delta y)^2}\right) \psi_{i,j+1}^n + \left(\frac{2}{(\Delta y)^2} + \frac{2}{\Delta t}\right) \psi_{i,j}^n + \left(-\frac{1}{(\Delta y)^2}\right) \psi_{i,j-1}^n \quad (5) \end{aligned}$$

And for the time with a half step: $\left(n + \frac{1}{2}\right) \Delta\tau = \frac{\Delta t}{2}$

$$\begin{aligned} \frac{\psi_{i,j}^{n+1} - \psi_{i,j}^{n+\frac{1}{2}}}{\frac{\Delta t}{2}} - \zeta_{i,j}^n &= \frac{\psi_{i+1,j}^{n+\frac{1}{2}} - 2\psi_{i,j}^{n+\frac{1}{2}} + \psi_{i-1,j}^{n+\frac{1}{2}}}{(\Delta x)^2} + \frac{\psi_{i,j+1}^{n+1} - 2\psi_{i,j}^{n+1} + \psi_{i,j-1}^{n+1}}{(\Delta y)^2} \Rightarrow \\ \Rightarrow \left(-\frac{1}{(\Delta y)^2}\right) \psi_{i,j+1}^{n+1} + \left(\frac{2}{(\Delta y)^2} + \frac{2}{\Delta t}\right) \psi_{i,j}^{n+1} + \left(-\frac{1}{(\Delta y)^2}\right) \psi_{i,j-1}^{n+1} &= \zeta_{i,j}^n + \left(-\frac{1}{(\Delta x)^2}\right) \psi_{i+1,j}^{n+\frac{1}{2}} + \left(-\frac{2}{(\Delta x)^2} + \frac{2}{\Delta t}\right) \psi_{i,j}^{n+\frac{1}{2}} + \left(-\frac{1}{(\Delta x)^2}\right) \psi_{i-1,j}^{n+\frac{1}{2}} \quad (6) \end{aligned}$$

Thus, the system of equations we conclude for equation (2), using the intermediate step, is:

$$\begin{cases} A_1 \psi_{i+1,j}^{n+\frac{1}{2}} + A_2 \psi_{i,j}^{n+\frac{1}{2}} + A_1 \psi_{i-1,j}^{n+\frac{1}{2}} = \zeta_{i,j}^n + B_1 \psi_{i,j+1}^n + B_2 \psi_{i,j}^n + B_1 \psi_{i,j-1}^n & (5) \\ C_1 \psi_{i,j+1}^{n+1} + C_2 \psi_{i,j}^{n+1} + C_1 \psi_{i,j-1}^{n+1} = \zeta_{i,j}^n + D_1 \psi_{i+1,j}^{n+\frac{1}{2}} + D_2 \psi_{i,j}^{n+\frac{1}{2}} + D_1 \psi_{i-1,j}^{n+\frac{1}{2}} & (6) \end{cases} \quad (III)$$

Where:

$$\begin{aligned}
A_1 &= \left(-\frac{1}{(\Delta x)^2} \right) , \quad C_1 = \left(-\frac{1}{(\Delta y)^2} \right) \\
A_2 &= \left(\frac{2}{(\Delta x)^2} + \frac{2}{\Delta t} \right), \quad C_2 = \left(\frac{2}{(\Delta y)^2} + \frac{2}{\Delta t} \right) \\
B_1 &= \left(-\frac{1}{(\Delta y)^2} \right) , \quad D_1 = \left(-\frac{1}{(\Delta x)^2} \right) \\
B_2 &= \left(\frac{2}{(\Delta y)^2} + \frac{2}{\Delta t} \right), \quad D_2 = \left(-\frac{2}{(\Delta x)^2} + \frac{2}{\Delta t} \right)
\end{aligned}$$

2.3 Discretion of Boundary Conditions

To be able to proceed with the construction of the solution algorithm, the discretization of the boundary conditions of the system (I) is also required. In section (1.1) the boundary conditions for the 4 variables of interest (u,v, ψ , ζ) were established. All that remains for the complete definition and discretization of the SS is the discretization of the 2nd partial derivative appearing in the SS of the vorticity.

Let's rewrite system (I) as a reminder:

$$\left\{ \begin{array}{l}
\text{Επάνω τοίχωμα : } \frac{\partial^2 \psi}{\partial x^2} = 0 \Rightarrow \zeta_{\text{τοιχωμα}} = -\frac{\partial^2 \psi}{\partial y^2} \\
\text{Κάτω τοίχωμα : } \frac{\partial^2 \psi}{\partial x^2} = 0 \Rightarrow \zeta_{\text{τοιχωμα}} = -\frac{\partial^2 \psi}{\partial y^2} \\
\text{Δεξιά τοίχωμα : } \frac{\partial^2 \psi}{\partial y^2} = 0 \Rightarrow \zeta_{\text{τοιχωμα}} = -\frac{\partial^2 \psi}{\partial x^2} \\
\text{Αριστερά τοίχωμα : } \frac{\partial^2 \psi}{\partial y^2} = 0 \Rightarrow \zeta_{\text{τοιχωμα}} = -\frac{\partial^2 \psi}{\partial x^2}
\end{array} \right. \quad (I)$$

Upper Wall

As the dimensions of our grid we previously defined the numbers of nodes in the 2 directions (nodx, nody). Writing the term at the penultimate node in column i and nody-1 row and expanding this term in a Taylor series we get: $(\psi_{i,nody-1})$

$$\begin{aligned}
\psi_{i,nody-1} &= \psi(i\Delta x, nody\Delta y - \Delta y) \\
&= \psi_{i,nody} - \frac{\partial \psi}{\partial y}(x, nody\Delta y)\Delta y + \frac{\partial^2 \psi}{\partial y^2}(x, nody\Delta y)\frac{(\Delta y)^2}{2} + O(\Delta y)^3
\end{aligned}$$

As we said during the definition of SS (1.1), by substituting this relation in the above equation and solving in terms of the 2nd derivative we have: $\frac{\partial \psi}{\partial y}(x, nody\Delta y) = U_w$

$$\frac{\partial^2 \psi}{\partial y^2}(x, nody\Delta y) = \frac{2(\psi_{i,nody-1} - \psi_{i,nody})}{(\Delta y)^2} + \frac{2U_w}{\Delta y} + O(\Delta y)$$

Therefore the 1st equation in system I to calculate the curvature in the upper wall becomes:

$$\zeta_{i,nody} = -\frac{\partial^2 \psi}{\partial y^2}(x, nody\Delta y) = -\frac{2(\psi_{i,nody-1} - \psi_{i,nody})}{(\Delta y)^2} - \frac{2U_w}{\Delta y}$$

Applying the same procedure for the remaining walls, the system (IV) is obtained:

$$\left\{ \begin{array}{l} \text{Upper Wall: } \zeta_{i,nody} = -\frac{2(\psi_{i,nody-1} - \psi_{i,nody})}{(\Delta y)^2} - \frac{2U_w}{\Delta y} \\ \text{Lower Wall : } \Rightarrow \zeta_{i,1} = \frac{2(\psi_{i,1} - \psi_{i,2} + \Delta y u_{i,1})}{(\Delta y)^2} \\ \text{Left wall : } \zeta_{1,j} = \frac{2(\psi_{1,j} - \psi_{2,j} - \Delta x v_{1,j})}{(\Delta x)^2} \\ \text{Right Wall : } \zeta_{nodx,j} = \frac{2(\psi_{nodx,j} - \psi_{nodx-1,j} + \Delta x v_{nodx,j})}{(\Delta x)^2} \end{array} \right. \quad (IV)$$

We have now discretized the equations that describe the flow and its SS. Therefore we can proceed to build the Algorithm for solving the above equations so as to calculate the flow.

3. PROCEDURE FOR CALCULATING FLOW FIELD

3.1 Relaxation Techniques

Before constructing the computational algorithm, we will explain the relaxation method that we will apply, in order to reduce the computational load, but also to increase the accuracy of the solution approach.

After we have calculated our solution for time (n+1), we apply an iterative process to improve our solution for this time level. By improvement we mean better convergence to the exact value of the solution. We start working from the node of the 2nd row and 2nd column (since the 1st row 1st column are known SS), and scan all the nodes of our grid. We write the discretized equations that express our flow field, and consider as unknown only the variable at the node for iteration (m+1). All other variables are assumed to be known at iteration step m.(i, j)

The above procedure for the variable (e.g. A) gives us the intermediate value. Using this value we calculate the value at the node from the equation: $\overline{A_{i,j}^{m+1}}. (i, j)$

$$A_{i,j}^{m+1} = A_{i,j}^m + \omega \left(\overline{A_{i,j}^{m+1}} - A_{i,j}^m \right) \quad (7)$$

Where ω is a relaxation factor and is usually chosen for each problem after trials, for our problem we set it equal to $\omega = 1.2$ when we are at large values of Re, so our technique is characterized as an under-relaxation technique. This choice of omega is due to the reduction of the large computing time we want to achieve. Now having the value for the m+1 iteration for the node, we proceed to the next node and apply the same procedure, except that where terms appear that refer to the values we calculated at the previous nodes, we enter the updated values $(i, j)(i + 1, j)A_{i,j}^{m+1}$.

This iterative process continues until convergence of the solutions is achieved for all grid nodes. That is, up to , where the error ε is defined by us. Once this process is completed we return to the ADI scheme and apply the procedures from the beginning for the next time step. $A_{i,j}^{m+1} - A_{i,j}^m < \varepsilon$

For our problem we will apply this technique at the end of the calculations for both the vorticity and the stream function. The application for both quantities of interest will be done at the end of each time step to improve the convergence. More specifically from the values we will have calculated using the ADI method, we will then apply the relationships:

$$\begin{aligned} (\zeta_{i,j}^n)^{m+1} &= (1 - \omega)(\zeta_{i,j}^n)^m + \omega \left(\overline{(\zeta_{i,j}^n)^{m+1}} \right) \\ (\psi_{i,j}^n)^{m+1} &= (1 - \omega)(\psi_{i,j}^n)^m + \omega \left(\overline{(\psi_{i,j}^n)^{m+1}} \right) \end{aligned}$$

Where the values with a dash above them are the values we got from the ADI method

3.2 Explicit Algorithm

Now we have all the necessary methods and procedures to be used and we are ready to build the computational algorithm. Due to the great complexity that appears in the calculation of the equations of our flow field, the steps of the algorithm will be fully analyzed, both with a description of the path and with the use of the equations that we will use.

In our grid and in the computational path we will follow, it moves in the direction of x and in the direction of y, or otherwise it expresses the column of the grid we are in and j the line. as coordinates will be written in the non-conventional format (lines – columns) $iji (i, j)$.

1. First we construct our mesh, the registers with which we will work (u,v,ψ, ζ), we define the necessary boundary conditions for the velocities in these registers. We also initialize these registers with zero initial values, so that they express the time t=0)
2. Stream Function Calculation (ψ)

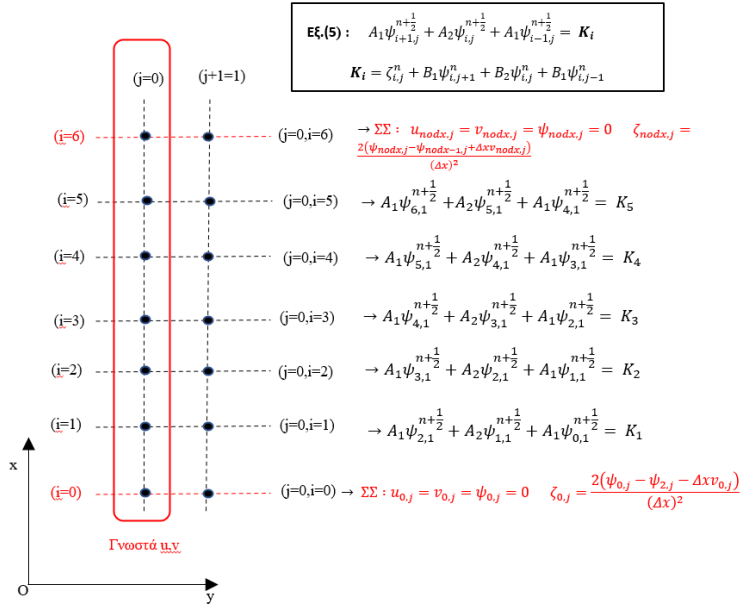
We calculate the system (III):

$$\begin{cases} A_1\psi_{i+1,j}^{n+\frac{1}{2}} + A_2\psi_{i,j}^{n+\frac{1}{2}} + A_1\psi_{i-1,j}^{n+\frac{1}{2}} = \zeta_{i,j}^n + B_1\psi_{i,j+1}^n + B_2\psi_{i,j}^n + B_1\psi_{i,j-1}^n & (5) \\ C_1\psi_{i,j+1}^{n+1} + C_2\psi_{i,j}^{n+1} + C_1\psi_{i,j-1}^{n+1} = \zeta_{i,j}^n + D_1\psi_{i+1,j}^{n+\frac{1}{2}} + D_2\psi_{i,j}^{n+\frac{1}{2}} + D_1\psi_{i-1,j}^{n+\frac{1}{2}} & (6) \end{cases} \quad (III)$$

- First keeping j constant (same line), we write equation (5) for all i (grid columns), except the 1st and last column. This process results in a tridiagonal system which is solved using the Thomas algorithm.
- We repeat the same process for all the lines except the 1st and the last (there we have the SS). Thus we end up having the values of the routin function for all nodes in the intermediate time step. $n + \frac{1}{2}$
- We repeat the same procedure for equation (6) with the difference that now we keep constant (same column) and write equation (6) for all j (rows) except the 1st and the last. We solve the resulting tridiagonal system with Thomas. i
- We repeat the same process for all the lines except the 1st and the last, so we end up with the values of the flow function for time $n+1$.

Before proceeding to the next step of the algorithm, we will give a small example of how to apply the above procedure. For example, for the 1st step of calculating , for a grid with 7 nodes we will

have the form shown in Figure 3. $\psi_{i,j}^{n+\frac{1}{2}}$



Shape3. Example of constructing a Tridiagonal register for the stram function

We notice in the figure above that applying equation (5) to the entire line gives us 5 equations. In the 1st and last equation we see that the terms are known because of SS,

thus a tridiagonal system is obtained which is solved for the 5 unknowns: . After solving this we can move on to the next j. $\psi_{6,1}^{n+\frac{1}{2}}, \psi_{0,1}^{n+\frac{1}{2}}, \psi_{1,1}^{n+\frac{1}{2}}, \psi_{2,1}^{n+\frac{1}{2}}, \psi_{3,1}^{n+\frac{1}{2}}, \psi_{4,1}^{n+\frac{1}{2}}, \psi_{5,1}^{n+\frac{1}{2}}$

For equation (6) of the 2nd step of our algorithm, we follow the same procedure.

3. Having now calculated the flow function for all positions of our grid for the time level (n+1), we apply these values to the SS of the system (IV) and calculate the SS for the

$$\text{vorticity at time (n+1).} \left\{ \begin{array}{l} \text{Upper Wall : } \zeta_{i,nody} = -\frac{2(\psi_{i,nody-1}-\psi_{i,nody})}{(\Delta y)^2} - \frac{2U_w}{\Delta y} \\ \text{Lower Wall : } \Rightarrow \zeta_{i,1} = \frac{2(\psi_{i,1}-\psi_{i,2}+\Delta y u_{i,1})}{(\Delta y)^2} \\ \text{Left wall : } \zeta_{1,j} = \frac{2(\psi_{1,j}-\psi_{2,j}-\Delta x v_{1,j})}{(\Delta x)^2} \\ \text{Right Wall : } \zeta_{nody,j} = \frac{2(\psi_{nody,j}-\psi_{nody-1,j}+\Delta x v_{nody,j})}{(\Delta x)^2} \end{array} \right. \quad (IV)$$

4. Calculation of Turbulence (g)

Now we can proceed to the calculation of the vorticity. We calculate the system (II):

$$\left\{ \begin{array}{l} A_{i,j}^n \zeta_{i-1,j}^{n+\frac{1}{2}} + B_{i,j}^n \zeta_{i,j}^{n+\frac{1}{2}} + C_{i,j}^n \zeta_{i+1,j}^{n+\frac{1}{2}} = D_{i,j}^n \zeta_{i,j-1}^n + E_{i,j}^n \zeta_{i,j}^n + F_{i,j}^n \zeta_{i,j+1}^n \quad (3) \\ AA_{i,j}^n \zeta_{i,j-1}^{n+1} + BB_{i,j}^n \zeta_{i,j}^{n+1} + CC_{i,j}^n \zeta_{i,j+1}^{n+1} = DD_{i,j}^n \zeta_{i-1,j}^{n+\frac{1}{2}} + EE_{i,j}^n \zeta_{i,j}^{n+\frac{1}{2}} + FF_{i,j}^n \zeta_{i+1,j}^{n+\frac{1}{2}} \quad (4) \end{array} \right. \quad (II)$$

- First we work with equation (3) and calculate all the terms on the right-hand side and the coefficients of the 3 unknowns on the left-hand side. Their values are considered known because they refer to the previous time step. So keeping as we did for the linear function, j constant, we write equation (3) for all but the 1st and the last. We apply the Thomas algorithm to the resulting tridiagonal system. i
- We apply the above procedure for all j except the 1st and the last. Thus we end up having calculated at all nodes the vorticity for the intermediate step $(n + \frac{1}{2})$
- We repeat these 2 steps for equation (4).
- Finally we have all values at all nodes for the vorticity at time n+1.

5. Relaxation technique

After calculating our field for time n+1, we proceed to apply relaxation techniques to improve accuracy. The relaxation will be applied only for the vorticity terms g.

We apply equation (7), using as intermediate values, the values given by the ADI method.

$$(\zeta_{i,j}^n)^{m+1} = (1 - \omega)(\zeta_{i,j}^n)^m + \omega \left((\zeta_{i,j}^n)^{m+1} \right) \quad (7\alpha)$$

$$(\psi_{i,j}^n)^{m+1} = (1 - \omega)(\psi_{i,j}^n)^m + \omega \left((\psi_{i,j}^n)^{m+1} \right) \quad (7\beta)$$

Step 5 is repeated for all points of our grid.

6. We have now calculated the vorticity and the stream function for our entire field at time $n+1$.

We repeat steps 2 to 5 until the condition is satisfied:

$$A_{i,j}^{n+1} - A_{i,j}^n \leq e$$

Where the error e you give us from the utterance The above condition must be satisfied for our entire flow field and only then can we say that we are in the steady state. $e = 10^{-4}$.

To calculate the error we have:

$$\varepsilon = \sum_{i,j=1}^{nodx,nody} (\zeta_{i,j}^{n+1} - \zeta_{i,j}^n)^2$$

We choose quadratic error so that, once the error value drops below unity, we have faster convergence. With the above definition of error we are essentially comparing the relative error that exists between 2 consecutive time points. As a verification of this criterion, we should point out that the same error calculation scheme is used by the commercial (and more famous) fluid mechanics problem solver ANSYS.

7. We calculate the speeds u , v from the relations:

$$u = \frac{\partial \psi}{\partial y} \quad v = -\frac{\partial \psi}{\partial x}$$

3.3 Results and Comparison

In this section the results are presented. The parameters of the computational application of the above algorithm are the following for all Reynolds numbers:

- Authentication Steps : $\Delta x = 0.01$, $\Delta y = 0.01$, $\Delta t = 10^{-4}$
- Convergence error: $\varepsilon = 10^{-4}$
- Relaxation factor : For , For $Re = 1 \rightarrow \omega = 1$ $Re = 100$ $\text{and } 500 \rightarrow \omega = 1.2$

From the above we see that we have 101 nodes at each address,

$$\text{Node Number} = 101 \times 101 = 10201$$

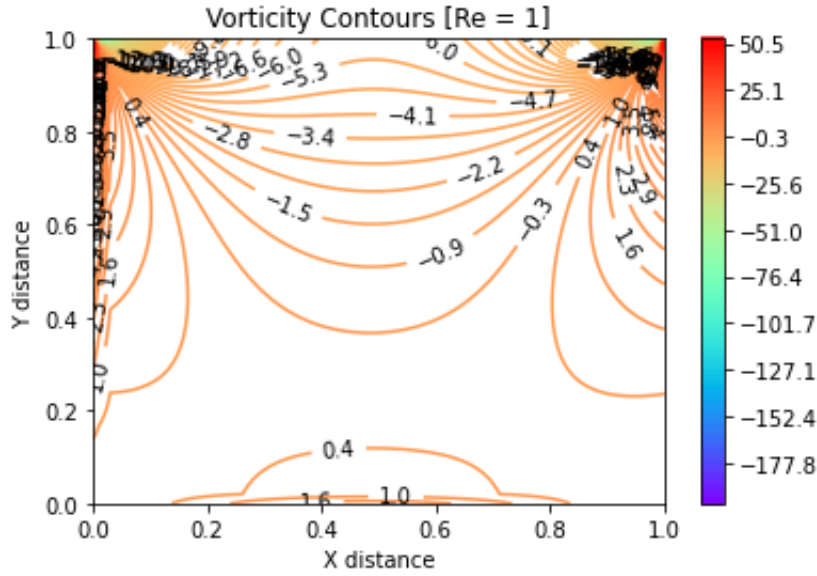
For the coloring of the charts, we choose the red color for the large values, and the blue for the smaller values, for the intermediate values the colors evolve in steps.

Based on these parameters we get the results presented below. Summarized in Table 1, we present the number of iterations and the time taken to compute the flow field for each Reynolds number.

Panel1. Number of Iterations and Run Time for different Reynolds

	$Re = 1$	$Re = 100$	$Re = 500$
Number of Repetitions	1470	6471	16236
Execution Time (sec)	355	1620	3899

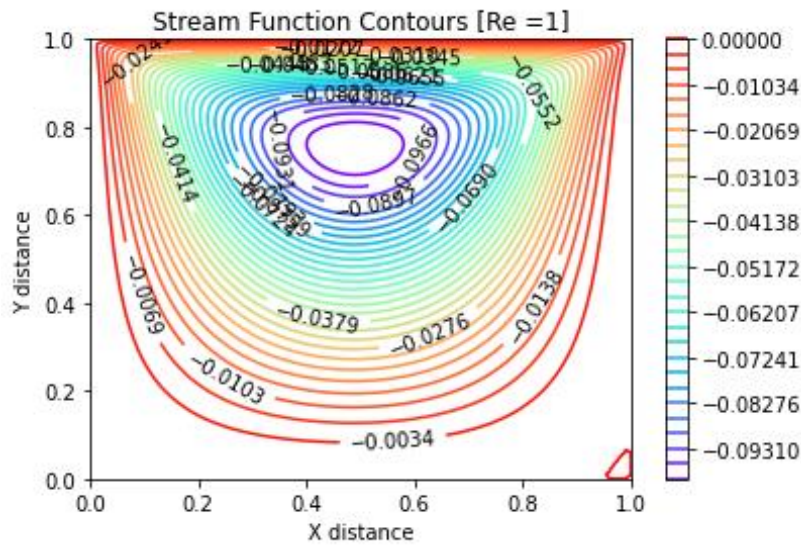
1) **Reynolds = 1**



Shape4. Vortex lines in a cavity of rectangular cross-section for $Re=1$

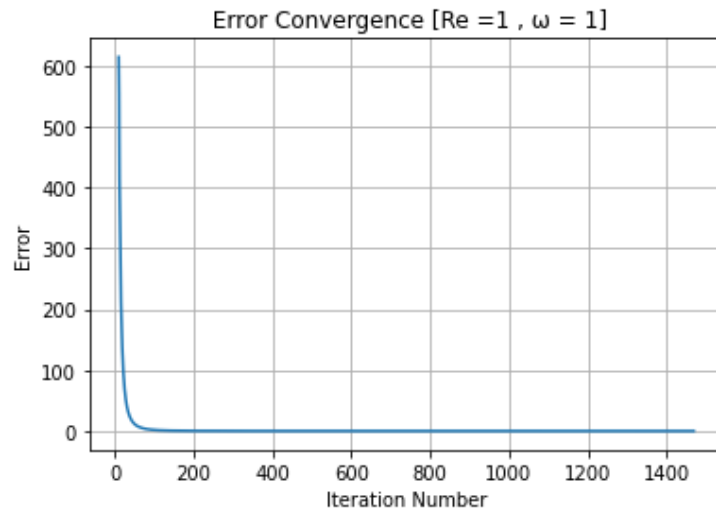
In Figures 4 to 6, the graphs for a Reynolds number equal to unity are presented. In Figure 4, we see the plot of isoheight curves for vorticity. In Figure 5, we see the raw lines and in Figure 6, we see the computational error and its evolution for each iteration. In these figures we also distinguish the corresponding values for the vorticity and flow lines at each level.

From these diagrams we can distinguish the highest values for the flow function that appear inside the cavity and the lowest that appear near the walls. Also from figure 4, we can see the different regions in the cavity, with positive and negative vorticity. The direction change of these vortices takes place at the walls.



Shape5. Flow lines in a cavity of rectangular cross-section for $Re=1$

For the error, we see that in the 1st iterations we have a sharp reduction, while afterwards the rate of reduction decreases dramatically. For the vorticity we visualize the isoheights for 400 levels while for the stream function for 30, this choice is made so that the levels of interest can remain distinct, so that we can compare the results.

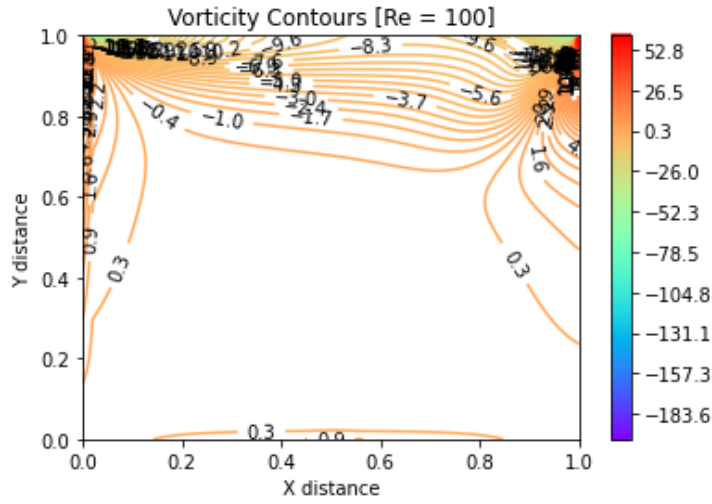


Shape6. Solution convergence error for Reynolds number = 1

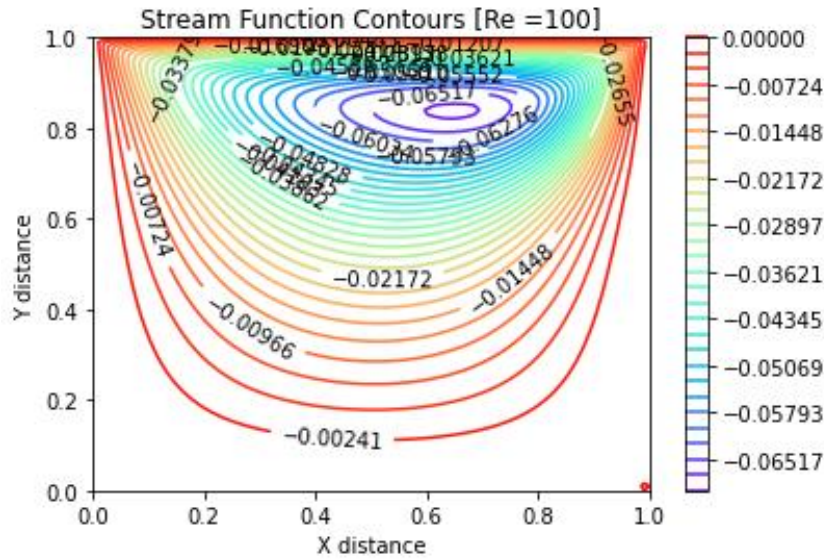
2) Reynolds = 100

In Figures 7 to 9, the plots are shown for a Reynolds number equal to 100. In Figure 7, we see the plot of the isoheight curves for the vorticity. In Figure 8, we see the raw lines and in Figure 9, we

see the computational error and its evolution for each iteration. In these figures we also distinguish the corresponding values for the vorticity and flow lines at each level.



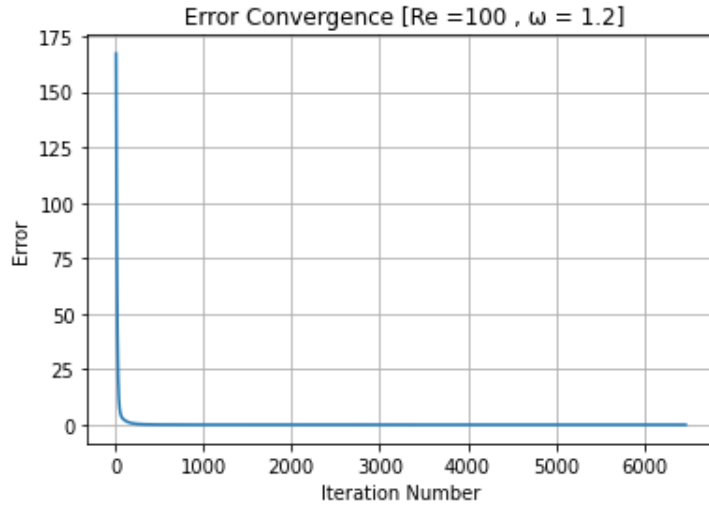
Shape7. Vortex lines in a cavity of rectangular cross-section for $Re=100$



Shape8. Flow lines in a cavity of rectangular cross-section for $Re=100$

For the error we observe the same behavior as before. From the values in table 1, we see the large increase in computational load (in time and iterations) in order to achieve convergence. To emphasize that in order to achieve better times for the number $Re=100$, we set the relaxation factor equal to 1.2 as opposed to previously which was unity.

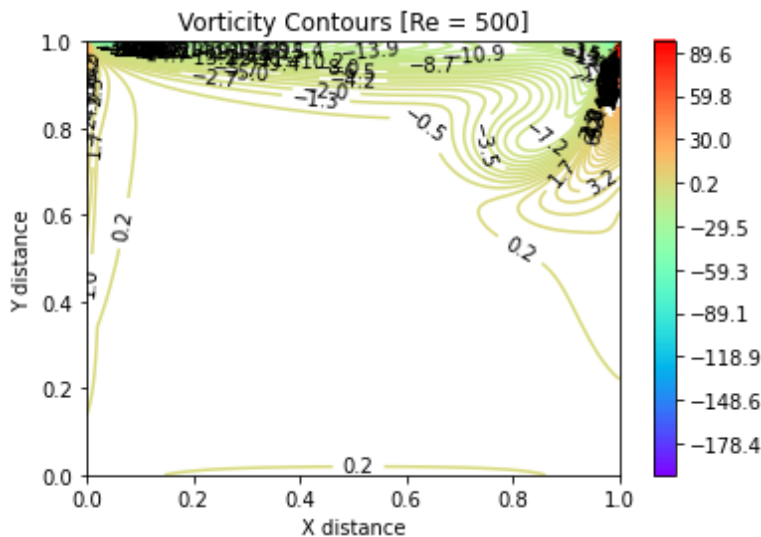
From Figure 8, we can see the high values we have for the rheological function, near the walls and its decrease as we approach the interior of the pit. Also from Figure 7, for the vorticity, we can see that the regions of intense vorticity are closer (clustered) to the walls than for $Re=1$.



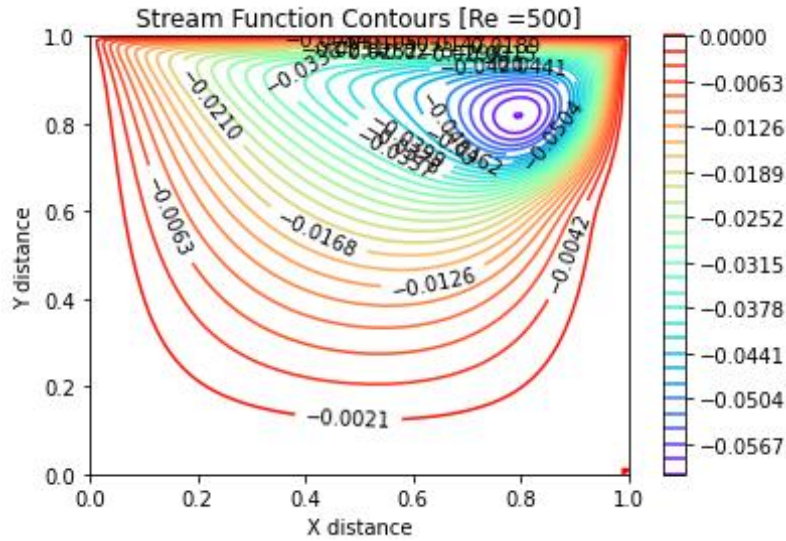
Shape9. Solution convergence error for Reynolds number = 100

3) Reynolds = 500

In Figures 10 to 12, the diagrams are shown for Reynolds number = 500. As the Re number increases we see that the values for the vorticity increase. From Figure 10 we can see that the main vortex has shifted to the right, towards the direction of movement of the upper wall. We can also see that the secondary vortices on the bottom and left walls have moved closer to the walls and the vorticity value on them has also decreased. In Figure 11, which shows the streamlines, the shift of the main vortex to the right is even more apparent. We still see that as the Re number increases, the absolute maximum values for the flow lines decrease.

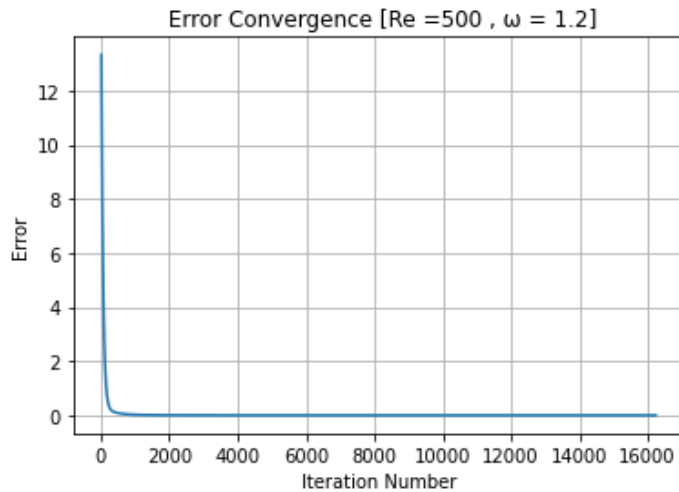


Shape10. Vortex lines in a cavity of rectangular cross-section for Re=500



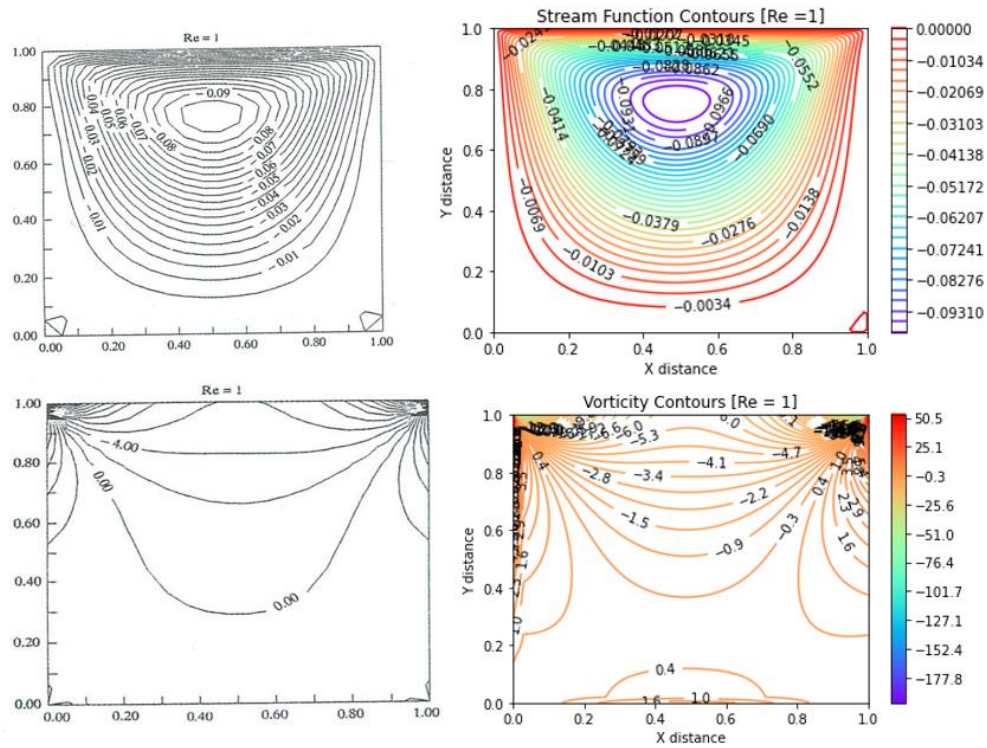
Shape11. Flow lines in a cavity of rectangular cross-section for $Re=500$

From Table 1, and from Figure 12 we can see that the number of iterations and the time it took for our solution to converge is very large compared to the solutions for smaller Re . We can see though that our error has the same behavior as before.



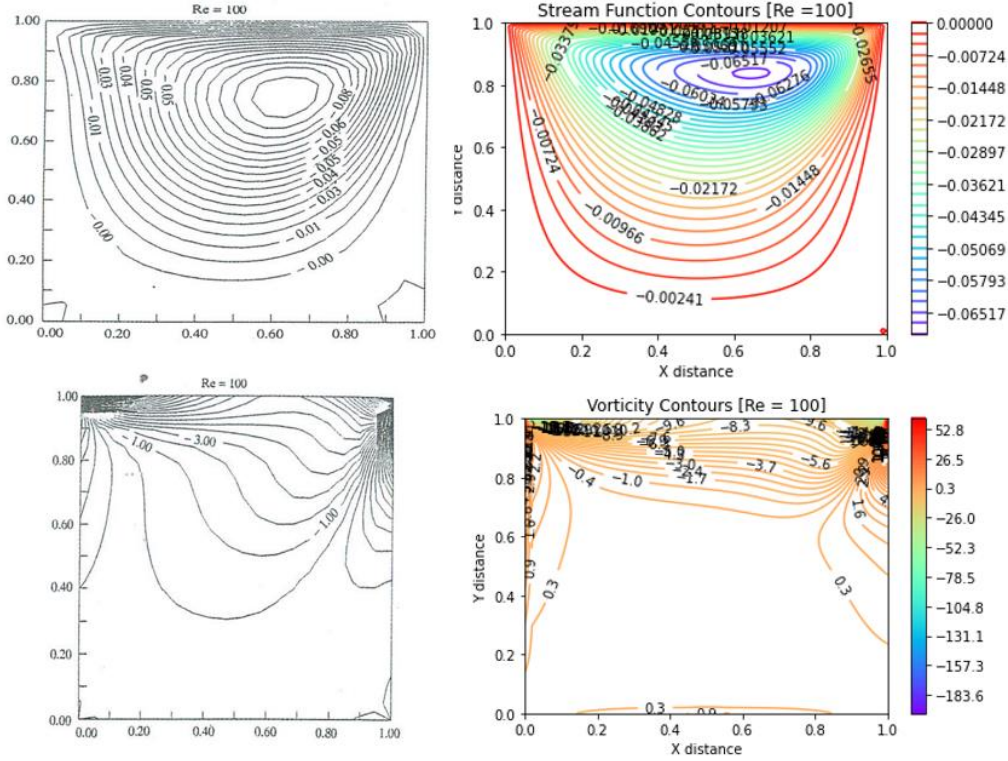
Shape12. Solution convergence error for Reynolds number = 500

To verify our calculated results, we compare the streamline diagrams and the vorticity diagrams for Reynolds numbers 1 and 100. Our diagrams will be compared with those given in the talk. Figures 13 and 14 show the charts for comparison.



Shape13. Comparison of ζ and ψ diagrams for Reynolds number =1

We see from the figure above that for the 2 diagrams, we could marginally say that they are identical. We can also observe that the values that can be seen in the left diagrams (pronunciation) can be observed in the corresponding positions in the right diagrams (calculated). Therefore for $Re=1$ the comparison of the results is very satisfactory.



Shape14. Comparison of ζ and ψ diagrams for Reynolds number = 100

From Figure 14, for $Re=100$ we see that the calculated diagrams are close to the behavior of the speech diagrams. For the stream lines it is obvious that the central gives shift to the right. Also from the values shown on the curves we can say that we have an identification of the values. For vorticity also the behavior is similar. In the pronunciation diagrams, of course, the curves appear to extend to the center of the pit. We lose these curves in the calculated diagrams due to the choice of the ζ levels that we visualize. In general, however, the prices in the corresponding positions appear to be the same.

The above, since we are not able to verify our results with experimental data, we can say that, by comparison with the speech diagrams, our code and the solution methodology, give satisfactory results and work correctly.

4. GRID INDEPENDENCE STUDY

In the 3rd question we are asked to make the grid independent. For mesh independence we will apply the sets of initial parameters for our mesh, presented in Table 2. The Reynolds number will be kept for all 3 dimensions of the mesh equal to unity ($Re=1$).

Panel2. Initial parameters for the grid independence study

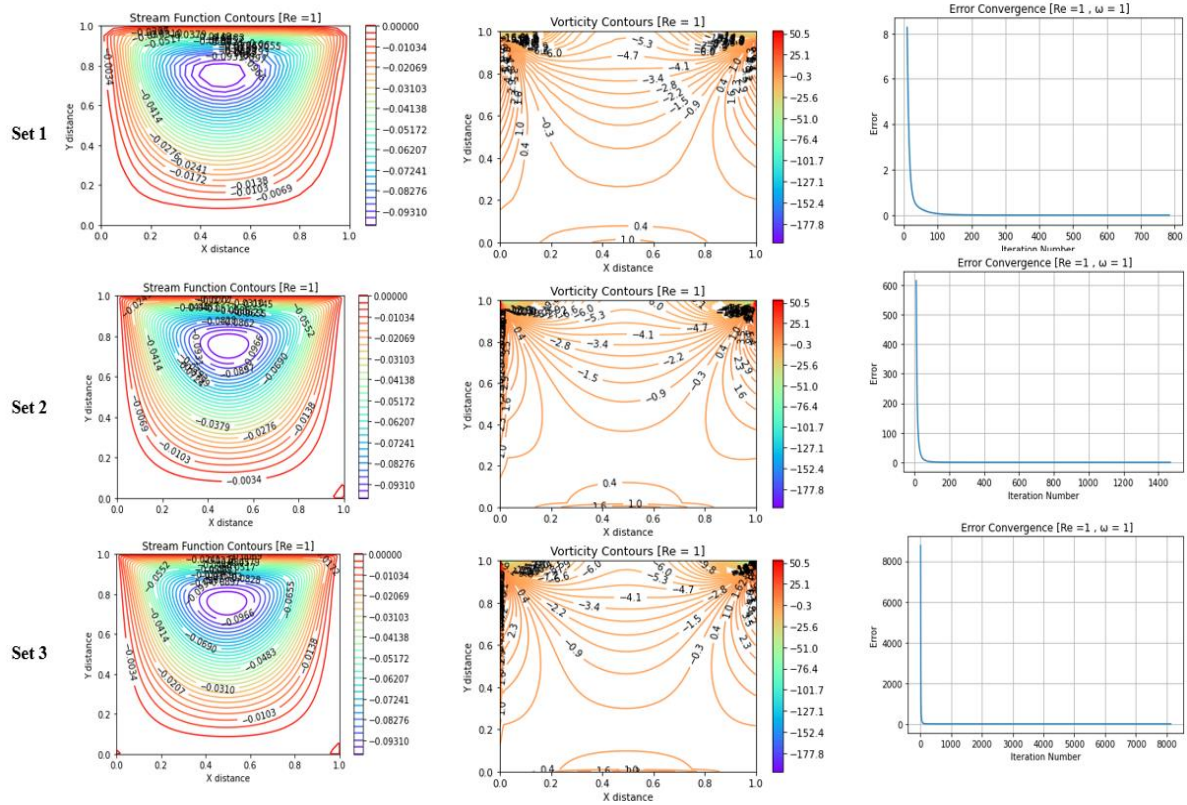
	Δx	Δy	Δt	Number of nodes
Set 1	$\Delta x = 0.05$	$\Delta y = 0.05$	$\Delta t = 10^{-4}$	441
Set 2	$\Delta x = 0.01$	$\Delta y = 0.01$	$\Delta t = 10^{-4}$	10201
Set 3	$\Delta x = 0.005$	$\Delta y = 0.005$	$\Delta t = 10^{-5}$	40401

Figure 15 below shows the comparison charts for the 3 sets of values. For the 3rd set from Table 2, we see that we dropped the time step by an order of magnitude because otherwise we did not converge to a solution. In addition, in Table 3, the convergence times needed for each set of parameters are also found.

Panel3. Number of iterations and Convergence time for grids of three different dimensions

	Iterations	Time (seconds)
Set 1	785	6.93
Set 2	1470	355
Set 3	8139	7243

Initially from Table 3, we see that increasing the dimensions of the grid, we have a very large increase in the computational time and burden for solving the rheological field. Specifically, we should point out that from the 1st to the 2nd set we have a doubling of repetitions and approximately 50 times longer execution time, while from the 2nd to the 3rd set we have a 5-fold increase in repetitions and approximately 200 times longer execution time. Before we proceed to analyze the plots, let us say that for smaller discretization steps of set 3, the computer failed to solve the problem and was leading to instability. Also for different steps Δx and Δy , the computational difficulty increases rapidly. ($\Delta x \neq \Delta y$)



Shape15. Comparison of grids of three different dimensions

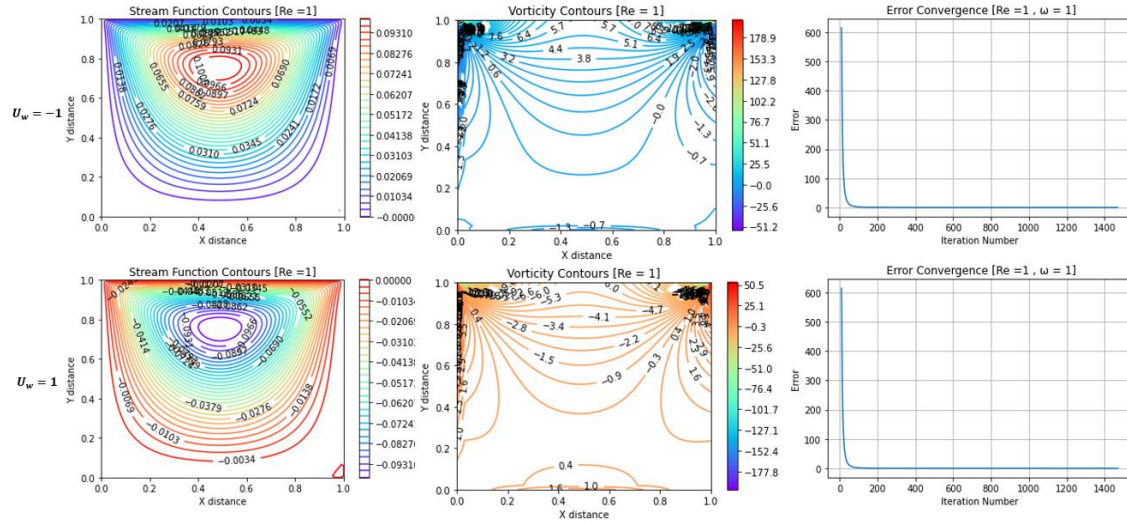
From the plots in Figure 15, we see that the variations from set of values to set of values are minimal. The overall image of the field can be captured satisfactorily even for small grid sizes. Therefore we can say that depending on the problem we are facing and the degree of accuracy of the results we are looking for, we should choose the corresponding grid approach. For the error, we also see from the last column of Figure 15, that for a large number of nodes in the grid, the error starts from very large values in relation to the other two grid dimensions. Finally to say that in case we had limited computing power and because the 3rd set of values shows an increased computational load, this could lead to a failure of the computational fluid mechanics application process.

5. SOLUTION WITH DIFFERENT BOUNDARY CONDITIONS

In the last question of the paper we are asked to change the direction of movement of the upper wall and solve the same problem. In particular we will solve the same problem only for Reynolds = 1 and compare with the results presented earlier.

5.1 Differentiate, Solve and Compare

In the code all we need to change is the speed value from 1 to -1. The results are presented in Figure 16. The top line of graphs in this figure includes the new calculated plots while the bottom one contains the plots presented in the previous sections. U_w



Shape16. Comparison of flow diagrams for different boundary conditions and $Re=1$

From the figure above we first distinguish the differentiation of colors. This differentiation is due to the fact that we color the larger values in red and the smaller values in blue. By changing the direction of the flow, we have a change of signs in the quantities to be calculated, as a result of which we see a different color visualization. For the error from the last column of plots in Figure 16, we see that it remains exactly the same for both problems. Regarding the solving time, we should mention that for the original problem we needed 355 seconds while for the differentiated one 380 seconds. The plots of the row lines and the vorticity show the same shape and a slight variation in the values of their curves with respect to the measure. We would expect the prices to change sign only. The difference in values can be due to calculation errors (since it is small) or to the values of the levels in which we set the iso-elevation curves to be displayed.

6. BIBLIOGRAPHY

1. Ferziger Peric - Computational Methods for Fluid Dynamics, 3rd Ed – 2002
2. Anderson-Computational-Fluid-Dynamics-McGraw-Hill-Science__Engineering__Math-1995
3. 'Computational Fluid Mechanics' course notes.